

# Inducing Anaesthesia via Exact Feedback Linearization control

Paul A. Pinte<sup>a</sup>\* Eva H. Dulf<sup>a</sup>\* Cristina I. Muresan<sup>a</sup>\*  
Clara M. Ionescu<sup>a</sup>\*

<sup>a</sup> *Department of Automation, Technical University of  
Cluj-Napoca, Memorandumului Street, no. 28, 400114 Cluj-Napoca,  
Romania, (e-mail: {Paul.Pinte, Eva.Dulf}@aut.utcluj.ro)*

<sup>\*\*</sup> *Ghent University, Department of Electromechanics, Systems and  
Metal Engineering, Research Group on Dynamical Systems and  
Control, Tech Lane Science Park 125, Zwijnaarde 9052, Belgium*

---

**Abstract:** The necessity of painless surgery and delivering an accurate dose of drug to induce anaesthesia to the patient is indubitable. Delivering a higher dose to the patient may lead to adverse effects and postoperative complications, while a lower dose obviously leads the patient to regain consciousness during the surgery and in extreme cases even to surgery failure. To overcome such complications during surgeries several research studies revolve around the design of a computer-controlled system to deliver an accurate dose of drug to induce anaesthesia. Therefore this paper aims to introduce an exact linearization of the drug administration model in anaesthesia, without losing too much information about the internal dynamics. This is realised by creating a linear map between the input and output. The control law uses this model and is designed to ensure performances of no overshoot and minimum steady-state error. The control loop is tested on a system with parametric uncertainties (related to patient intra/inter-variability). The simulation results validate the proposed approach and demonstrate its robustness.

*Keywords:* exact linearization via feedback, depth of hypnosis, uncertain systems, closed loop control of anaesthesia.

---

## 1. INTRODUCTION

It is obvious the need of anaesthesia in the context of surgery and medicine in general. With the progress of technology and system control engineering a computer based drug dosing of general anaesthesia management can be achieved. One way to tackle anaesthesia is by controlling the Depth of Hypnosis, defined as a specific state of unconsciousness. In the present research, the Bispectral Index (BIS) is used as an accurate estimation of the level of unconsciousness Soltesz et al. (2020). This choice is based on the fact that dedicated sensors exist to measure the BIS signal. Having an accurate measurement, the feedback is ensured for the control loops in this anaesthesia process. This will help anaesthesiologist in the first stage by offering information in any point of the process. It can act as a digital twin of the anaesthesiologist. The BIS signal is considered 100 % for a fully awake patient and decreases towards 0%, a state of no cortical activity, due to the administration of Propofol. In most clinical interventions, a BIS signal of 50% is considered suitable for surgery, but the actual value can vary in a range from 40% to 60% C. Rosow (2001).

The modelling of drug administration in anaesthesia can be realised by Pharmacokinetics- **PK** part that discusses the kinetics of the drug, or the rate of transfer between different compartments and Pharmacodynamics - **PD** that represents the effect of drug concentration on the depth of

Hypnosis -**DoH** [Al-Rifai and Mulvey (2016) Blussé van Oud-Alblas et al. (2019) Minto et al. (1997)].

Multiple control strategies are developed for anaesthesia in existing literature. For example in Morley et al. (2000) a closed loop control strategy is presented with the BIS being the control target, while in Merigo et al. (2019) an optimal PID controller is proposed. In all cases the process is linearised by using approximation methods of the model [Beck (2015), Kharisov et al. (2012), Struys et al. (2004), Zhusubaliyev et al. (2015)].

The primary focus of the present paper lies in the feedback linearization approach, which aims to maintain essential information about the internal dynamics while establishing a linear mapping between the input and output.

The present paper is structured as follows: Part 2 describes the mathematical model, while part 3 discusses the feedback linearization of the BIS model as the theoretical core of the paper. Section 4 includes the simulation results with concluding remarks given in the final section of the paper.

## 2. MATHEMATICAL MODEL

The mathematical model will portray the dynamics between the input  $u(t)$  as the amount of Propofol and the output  $y(t) \doteq BIS(t)$  as the measurable Bispectral Index. In this paper the next general form of the system will be considered:

$$\Sigma : \begin{cases} \dot{\mathbf{x}} = f(\mathbf{x}) + g(\mathbf{x})u(t) + p(\mathbf{x})d(t) \\ y = h(\mathbf{x}), \end{cases} \quad (1)$$

where  $\mathbf{x} \in \mathbb{R}^4$ ,  $\mathbf{x} = [x_1, x_2, x_3, x_e]^\top$  are the states of the system that represent the concentration of the drug in the compartments of the model and  $x_i[mg/ml]$ ,  $f(\mathbf{x})$  is the vectorial function that defines the dynamics of  $\dot{\mathbf{x}}$ ,  $g(\mathbf{x})$  will map the input  $u(t)$  onto  $\mathbf{x}$ , as well the function  $p(\mathbf{x})$  does to the exogenous uncontrollable input  $d(t)$ . The latter one is considered to be the disturbance, which refers to any external influence or change that affects the behaviour of the internal states or the output function. For the purposes of the current paper we will make the assumption of  $d(t) \equiv 0$ . The model is a Pharmacokinetics-Pharmacodynamics **PK-PD** compartmental model used multiple times throughout literature Gambús and Trocóniz (2015), Blussé van Oud-Alblas et al. (2019). For the purposes of the present paper the model from the open source simulator will be used Ionescu et al. (2021), as such let us define the vectorial function that gives the states of the model from (1):

$$f(\mathbf{x}) = \begin{bmatrix} -c_1x_1(t) + k_{21}x_2(t) + k_{31}x_3(t) \\ k_{12}x_1(t) - k_{21}x_2(t) \\ k_{13}x_1(t) - k_{31}x_3(t) \\ k_{1e}x_1(t) - k_{e0}x_e(t) \end{bmatrix}, \quad (2)$$

where  $c_1 = k_{10} + k_{12} + k_{13}$ . Each of the constant elements  $k_{ij}$ ,  $i \neq j$  convey an information regarding the transfer rate of drug concentration within the states of the system. With the input mapping function onto (2) as  $g(\mathbf{x}) = [1 \ 0 \ 0 \ 0]^\top$  and the nonlinear output function that also describes the **BIS** as the next Hill function:

$$h(\mathbf{x}) = E_0 - E_m \frac{x_e(t)^\gamma}{C_{50}^\gamma + x_e(t)^\gamma}, \quad (3)$$

in this case  $h(\mathbf{x}) = BIS(t)[\%]$ . From this it can be stated that the model is a nonlinear one, given that the output function is strongly nonlinear.

### 3. FEEDBACK LINEARIZATION OF BIS MODEL

This section provides details regarding the mathematical tools that are needed to construct a linear map between Propofol input and BIS output. We have seen in the previous section, that as many other systems, the model is nonlinear, considered to be a single-input and single-output **-SISO** system, with this section the aim is to analytically construct a control law  $u(t)$  in such a way that we cancel out the nonlinearities. In the following paragraphs all the steps towards the goal will be discussed.

#### 3.1 Diffeomorphism Transformation

As shown in Isidori (1985), there is a need for a suitable change of coordinates made in such manner that the system in the new basis is in normal form. Moving further, let us define the relative degree  $\rho$  around a vicinity of a point  $\mathbf{x}^0$  for the nominal input affine system (1), which is given by the system described by Lie derivative relations:

$$\begin{cases} L_g L_f^k h(\mathbf{x}) = 0, \forall \mathbf{x} \in \mathcal{V}(\mathbf{x}^0), k < \rho - 1 \\ L_g L_f^{\rho-1} h(\mathbf{x}) \neq 0 \end{cases}, \quad (4)$$

where  $L_f h(\mathbf{x})$  is the Lie derivative of the nonlinear output function  $h(\mathbf{x})$  with respect to the vector field  $\mathbf{x}$  along the vectorial trajectory of  $f(\mathbf{x})$ , all evaluated within the radius of the neighbourhood  $\mathcal{V}(\mathbf{x}^0)$ . If one does not want to embark into solving the Lie derivative system predominantly due to the intrinsic complexity of the equations involved, the relative degree can be found by other means.

*Proposition 1.* The relative degree of the system of form (1) is the number of times one has to differentiate the output  $h(\mathbf{x})$  with respect to time until the value of the input appears in an explicit form ( $u(t)$  is directly used or referenced), the relative degree will be equivalent to the order of the derivative where this holds.

For the system (1) let us compute the relative degree:

$$\begin{aligned} \frac{dh}{dt} &= -E_m \gamma x_e(t)^{\gamma-1} \frac{k_{1e}x_1(t) - k_{e0}x_e(t)}{(C_{50}^\gamma + x_e(t)^\gamma)^2} \\ \frac{d^2h}{dt^2} &= -\frac{E_m \gamma (\gamma - 1) (k_{1e}(-c_1x_1 + k_{21}x_2 + k_{31}x_3 + u))}{(C_{50}^\gamma + x_e(t)^\gamma)^3} \\ &\quad + \frac{E_m \gamma^2 (k_{1e}(-c_1x_1 + k_{21}x_2 + k_{31}x_3 + u))}{(C_{50}^\gamma + x_e(t)^\gamma)^2} + \mathcal{Q}(\mathbf{x}) \end{aligned} \quad (5)$$

where  $\mathcal{Q}(\mathbf{x})$  are other terms in which  $u(t)$  does not appear. Paying attention to the second time derivative (5) the input  $u(t)$  appears in an explicit form therefore the relative degree  $\rho = 2$ . It is easy to see that for our case the relative degree is less than the order of the system ( $\rho = 2 < n = 4$ ), this implies that some zero dynamics or internal dynamics will be present. With this in mind we consider the following coordinate transformation:

$$\mathbf{z} = \Phi(\mathbf{x}) = \begin{bmatrix} \phi_1(\mathbf{x}) \\ \phi_2(\mathbf{x}) \\ \vdots \\ \phi_n(\mathbf{x}) \end{bmatrix}, \quad (6)$$

where  $\mathbf{z} \in \mathbb{R}^n$  and the mapping  $\Phi(\mathbf{x}) = \mathbf{z}$  should be a diffeomorphism - i.e. for  $\Phi(\mathbf{x})$  exists  $\Phi^{-1}(\mathbf{z})$  such that  $\Phi(\mathbf{x}), \Phi^{-1}(\mathbf{z}) \in \mathcal{C}^\infty$ , and the Jacobian matrix  $\frac{\partial \Phi(\mathbf{x})}{\partial \mathbf{x}}|_{\mathbf{x}^0}$  is non-singular. The most important propriety of the change of coordinates is to be a bijective map.

Having a lower relative degree the transformation will be constructed as follows: the first 2 elements of the diffeomorphism are given by the first  $\rho - 1 = 1$  Lie derivatives of the output function with respect to vector field  $\mathbf{x}$  and along the vector trajectory of  $f(\mathbf{x})$ , and to complete the dimensionality two functions  $\phi_3(\mathbf{x}), \phi_4(\mathbf{x})$  are added and will be discussed in the following sections. Therefore the local coordinates change will be as in (7),

$$\mathbf{z} = \Phi(\mathbf{x}) = \begin{bmatrix} h(\mathbf{x}) \\ L_f h(\mathbf{x}) \\ \phi_3(\mathbf{x}) \\ \phi_4(\mathbf{x}) \end{bmatrix}. \quad (7)$$

The first 2 coordinates are given by:

$$\begin{aligned} z_1 = h(\mathbf{x}) &= E_0 - E_m \frac{x_e(t)^\gamma}{C_{50}^\gamma + x_e(t)^\gamma} \\ z_2 = \langle \nabla h, f(\mathbf{x}) \rangle &= -\frac{E_m \gamma x_e(t)^{\gamma-1}}{(C_{50}^\gamma + x_e(t)^\gamma)^2} \cdot (k_{1e}x_1(t) - k_{e0}x_e(t)) \end{aligned}$$

To complete the diffeomorphism  $\Phi$ , we have to find two functions  $\phi_3(\mathbf{x}), \phi_4(\mathbf{x})$  such that:

$$L_g \phi_i(\mathbf{x}) = 0, \quad i \in \{3, 4\}, \quad \forall \mathbf{x} \in \mathcal{V}(\mathbf{x}^0).$$

Let us make the next notations:

$$\alpha(\mathbf{x}) = \langle \nabla L_f^{\rho-2} \langle \nabla h(\Phi^{-1}(\mathbf{z})), f \rangle, g \rangle \doteq L_g L_f^{\rho-1} h(\Phi^{-1}(\mathbf{z}))$$

$$\beta(\mathbf{x}) = L_f^{\rho-1} \langle \nabla h(\Phi^{-1}(\mathbf{z})), f \rangle \doteq L_f^{\rho} h(\Phi^{-1}(\mathbf{z}))$$

$$q_i(\mathbf{z}) = \langle \nabla \phi_i(\Phi^{-1}(\mathbf{z})), f \rangle = L_f \phi_i(\Phi^{-1}(\mathbf{z})), \quad i = \overline{1, 4},$$

The key propriety of this transformation stands in its derivative with respect with time, such as if the computation is made the normal form of the system reveal itself and it can be seen in (8). In this new form of the system the dynamics, including the nonlinear terms, are isolated with the input function, now  $u(t)$  can be picked in such a way that those terms cancel each other out.

This will convey a linear map between input  $u(t)$  and output  $y(t)$ .

$$\Phi(\dot{\mathbf{x}}) = \dot{\mathbf{z}} = \begin{bmatrix} \beta(\mathbf{z}) + \alpha(\mathbf{z}) \cdot u(t) \\ \text{---} \\ q_3(\mathbf{z}) \\ q_4(\mathbf{z}) \end{bmatrix}. \quad (8)$$

Therefore, the new coordinates are defined with a bijective map between the two:  $\mathbf{x} \xleftrightarrow[\Phi(\mathbf{x})]{\Phi^{-1}(\mathbf{z})} \mathbf{z}$ .

### 3.2 Zero Dynamics

In examining equation (8), it becomes evident that there exists a partial transformation of coordinates due to the relative degree being less than the system's order. This transformation introduces two supplementary functions denoted as  $q_i(\mathbf{z})$ ,  $i = \overline{1, 4}$ . This yields that the system has 2 internal states, that lack of effect into the output, the dynamics of those internal states will be called *zero dynamics* and to fulfil the purposes of this paper an analysis is clearly needed. Let us split the state vector in the new coordinates into two parts

$$\mathbf{z} = \begin{bmatrix} \zeta \\ \text{---} \\ \eta \end{bmatrix}, \quad (9)$$

where  $\zeta \in \mathbb{R}^2$  is the sub-state vector that contains the main states of the system that were part of (7) and  $\eta \in \mathbb{R}^2$  represents the sub-state vector containing the internal states and they can be seen in (8). We can make a choice for  $\phi_i(\mathbf{x})$   $i = 3, 4$  with the constraint that  $\Phi(\mathbf{x})$  will still be a diffeomorphism, the most logical choice is to include the exact states that were not included in the transformation, therefore:  $\phi_3(\mathbf{x}) = x_2$  and  $\phi_4(\mathbf{x}) = x_3$ .

Now the dynamics of the system will be described by differentiating  $\mathbf{z}$ :

$$\Psi : \begin{cases} \dot{\mathbf{z}} = \begin{bmatrix} \dot{\zeta} \\ \text{---} \\ \dot{\eta} \end{bmatrix} = \Phi(\dot{\mathbf{x}}), \\ y = z_1(t). \end{cases}$$

As the name suggests the influence of internal dynamics of the system appears in the case of zeroing the output. In the literature this problem is stated as finding all pairs of  $(\mathbf{x}^0, u^0)$  such that the relation (10) holds:

$$\Psi : \begin{cases} \Phi(\dot{\mathbf{x}})|_{(\mathbf{x}^0, u^0)} \\ y(t) \equiv 0. \end{cases} \quad (10)$$

A clear solution is  $(0, 0)$ , but we want to exclude the trivial pair. The normal form of the system give us the relation  $y(t) = z_1(t) = 0 \Rightarrow \dot{z}_1 = \dot{z}_2 = 0$ , from this is easy to observe the only dynamics are given by  $\phi_3(\mathbf{x}) = x_2$  and  $\phi_4(\mathbf{x}) = x_3$ . Therefore the evolution of  $(\Psi)$  is given by  $\eta$  as all the states  $\zeta \equiv 0$  with  $\dot{\eta} = q(0, \eta)$ . With this in mind it can be stated a new relation for  $q_3(\mathbf{x})$  given by the Lie derivatives:

$$\begin{aligned} q_3(\mathbf{z}) &= L_f \phi_3(\Phi^{-1}(\mathbf{z})) = \langle \nabla \phi_3, f(\mathbf{x}) \rangle \\ &= \begin{bmatrix} \frac{\partial x_2}{\partial x_1} & \frac{\partial x_2}{\partial x_2} & \frac{\partial x_2}{\partial x_3} & \frac{\partial x_2}{\partial x_4} \end{bmatrix} \cdot f(\mathbf{x}) = \dot{x}_2. \end{aligned} \quad (11)$$

In the same manner, we have:

$$q_4(\mathbf{z}) = L_f \phi_4(\Phi^{-1}(\mathbf{z})) = \langle \nabla \phi_4, f(\mathbf{x}) \rangle = \dot{x}_3. \quad (12)$$

as such, the zero dynamics can be stated as follows

$$\dot{\eta} = \begin{bmatrix} q_3 \\ q_4 \end{bmatrix} = \begin{bmatrix} \dot{x}_2 \\ \dot{x}_3 \end{bmatrix},$$

and the system  $\Psi$  in its explicit normal form is:

$$\Psi : \begin{cases} \dot{z}_1 = z_2 \\ \dot{z}_2 = \beta(\mathbf{z}) + \alpha(\mathbf{z}) \cdot u(t) \\ \dot{\eta} = q(\zeta, \eta) \\ y = z_1 \end{cases}. \quad (13)$$

The most important characteristic of the dynamics, is it's stability, therefore we focus on the subsystem  $\dot{\eta}(t)$ . In Isidori (1985) it was shown that computing the trajectory of the internal states taking a linear approximation of **the newly formed sub-system for internal dynamics** are interchangeable. Starting with the system in normal form presented in (13) the linear approximation of the zero dynamics when  $\eta = 0$  is given by the Jacobian matrix:

$$\begin{aligned} A_{nc} &= \left[ \frac{\partial q}{\partial \eta} \right] |_{(\zeta, \eta)=0} = \begin{bmatrix} \frac{\partial q_3}{\partial x_2} & \frac{\partial q_3}{\partial x_3} \\ \frac{\partial q_4}{\partial x_2} & \frac{\partial q_4}{\partial x_3} \end{bmatrix} |_{(\zeta, \eta)=0} \\ &= \begin{bmatrix} \frac{\partial}{\partial x_2} (k_{12}x_1 - k_{21}x_2) & \frac{\partial}{\partial x_3} (k_{12}x_1 - k_{21}x_2) \\ \frac{\partial}{\partial x_2} (k_{13}x_1 - k_{31}x_3) & \frac{\partial}{\partial x_3} (k_{13}x_1 - k_{31}x_3) \end{bmatrix} \\ &= \begin{bmatrix} -k_{21} & 0 \\ 0 & -k_{31} \end{bmatrix}. \end{aligned} \quad (14)$$

The eigenvalues of the companion matrix of the vector  $\eta$  are the roots of the characteristic polynomial correspondent with the zeros of the transfer function if one were to linearize around the equilibrium point  $\mathbf{x} = 0$ . As stated before,  $\dot{\eta} = A_{nc}\eta$ , thus when the system is in a state of zeroing the output all of the states of the system  $(\Psi)$  will evolve on the subset:

$$\mathcal{Z}^* = \{\mathbf{x} \in \mathbb{R}^4 : h(\mathbf{x}) = L_f h(\mathbf{x}) = 0\}, \quad (15)$$

with the dynamics dictated by  $\eta$  and, because the eigenvalues  $\lambda_1 = -k_{21}, \lambda_2 = -k_{31} \in \mathbb{C}_-$  the set  $\mathcal{Z}^*$  is a

stable set. Moreover it is a smooth manifold of dimension 2 giving a mathematical assurance that the computation of a diffeomorphism holds even in the case of zeroing the output.

The state feedback is considered as:

$$u^*(t) = \frac{-L_f^\rho h(\mathbf{x})}{L_g L_f^{\rho-1} h(\mathbf{x})} = \frac{-L_f^2 h(\mathbf{x})}{L_g L_f h(\mathbf{x})}. \quad (16)$$

If  $\mathbf{x} \in \mathcal{Z}^*$  and  $u(t) = u^*(t)$ , the vector field that gives the original orthonormal vector basis can be denoted as in (17).

$$f^*(\Phi^{-1}(\mathbf{z})) = f(\Phi^{-1}(\mathbf{z})) + g(\Phi^{-1}(\mathbf{z})) \cdot u^*(t), \quad (17)$$

this gives a closed-loop relation described by (18)

$$\Phi^{-1}(\dot{\mathbf{z}}) = f^*(\Phi^{-1}(\mathbf{z})), \quad (18)$$

with the very helpful propriety that if its initial conditions are on the smooth manifold  $\mathcal{Z}^*$  it is guaranteed that they will evolve onto the same manifold-closed path with a trajectory governed by  $A_{nc}$ . As the final step towards analysing the zero dynamics of the system, the subsequent values for  $A_{nc}$  are extracted from Ionescu et al. (2021):

$$A_{nc} = \begin{bmatrix} -0.0735 & 0 \\ 0 & -0.0035 \end{bmatrix}; \eta_0^{(i)} = \begin{bmatrix} \mathcal{N}(0, 30) \\ \mathcal{N}(0, 30) \end{bmatrix}, i = \overline{1, 40}$$

where  $\mathcal{N}(0, 30)$  is the normal distribution with the mean  $\mu = 0$  and standard deviation  $\sigma = 30$ , this will result in random initial conditions with values inside the interval  $[-30, 30]$ . The objective is to showcase the internal stability of the system irrespective of the initial conditions, hence the case of 40 random initial conditions. The evolution of the internal states can be seen in Fig. 1, it also can be observed that one state is faster than the other, however both will eventually evolve towards the equilibrium value of 0.

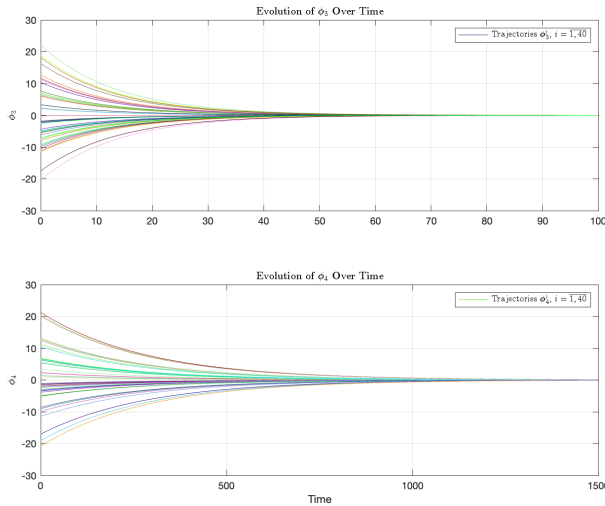


Fig. 1. The evolution of zero dynamics

### 3.3 Compensation of residual Non-Linearities

From the previous section one can denote that for  $u = u^*$  the system will be stabilised even at the zeroing of the output situation, but much more than that the system

will become linear because the input will cancel out the nonlinearities from the  $\rho^{th}$  state. As for the analytical expression the input can be rewritten as:

$$u = \frac{1}{\alpha(\zeta, \eta)} (-\beta(\zeta, \eta) + v(t)), \quad (19)$$

where  $v$  is defined as the new exogenous input for the new system. However a common problem arises: the limits of the control signal. For (19) Isidori has proven that  $\alpha(\zeta, \eta) \neq 0$  therefore excluding the situation of boundless input. But, the problem of an infeasible signal remains.

To align our theoretical analysis with the real world application a saturation was added to the values of  $u(t)$ , in order to not lose the generality let us define  $u_{min}$  and  $u_{max}$  as the minimal and maximal values for the input  $u$ , therefore

$$u = \text{sat}\left\{\frac{1}{\alpha(\zeta, \eta)} (-\beta(\zeta, \eta) + v(t)), u_{min}, u_{max}\right\} \quad (20)$$

By its definition a saturation added in the system is a powerful nonlinear element, however given that we assumed that the system is input-affine the nonlinear terms will be compensated by other means. One method is to artificially change the operation point towards a point where the saturation element does change the values of  $u$ .

### 3.4 Control Trajectory

As it has been presented, the internal states can be excluded from the control strategy if their dynamics are stable which holds for our case because they do not affect the output. If the inner loop is closed the system will become a  $2^{nd}$  order linear, fully controllable and observable system. It is worth mentioning that the internal states are correspondent with the uncontrollable states of the system if a linear approximation around an equilibrium point is taken.

Now let us tackle the problem of output tracking where output  $y$  has to follow a certain trajectory  $y_{ref}$ . This is the scope of the exogenous input  $v(t)$  from the equation (19). Considering the relative degree  $\rho = 2$ , the usual method of describing  $v(t)$  is by the relation:

$$v(t) = y_r^{(2)}(t) - \sum_{j=1}^2 k_{j-1}(z_i(t) - y_r^{(j-1)}(t)), \quad (21)$$

where  $y_r^{(j)}(t)$  is the  $j^{th}$  derivative of the reference,  $z_i$  are the states of the linear system, and  $k_j \in \mathbb{R}$  are the controller's parameters which should be designed. This structure is perfect for a state-feedback framework from which all  $k_j$  elements can be found, such an example was presented in a previous paper Pintea and Mihaly (2023) applied on a different model, however for the purposes of the present paper a different structure, **PD** structure is used.

After all this considerations, the inner closed-loop system after the exact linearization process can be written as:

$$\Psi_c : \begin{cases} \dot{\zeta} = A_c \zeta + B_c v \\ y = C_c \zeta. \end{cases} \quad (22)$$

with  $\zeta \in \mathbb{R}^2$  being the linear and controllable vector state,  $A_c \in \mathbb{R}^{2 \times 2}$ ,  $B_c \in \mathbb{R}^2$ ,  $C_c \in \mathbb{R}^{1 \times 2}$  being the matrices of

controllable canonical form. The transfer function of the system becomes a double integrator between  $v(t)$  and  $y(t)$

$$H(s) = \frac{1}{s^2}. \quad (23)$$

With this any suitable linear controller can be designed in order to impose feasible performances. Given the double integrator, a PD controller with a filter as in (24) is proposed. This will increase the phase margin and decrease the time response of the closed loop system.

$$H_{PD}(s) = \frac{k_d \cdot s}{T_f \cdot s + 1} \quad (24)$$

The process as a whole that the paper presents can be described in a few steps:

- Diffeomorphism Transformation
- Compute  $u(t)$  and close the loop
- Design a controller for the linear inner closed loop

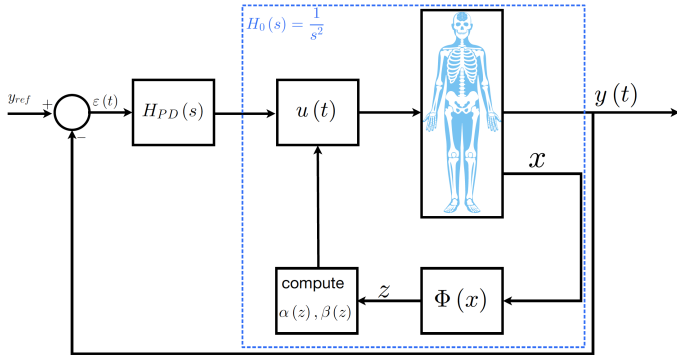


Fig. 2. Block Diagram of the System

This process can be seen in Fig. 2, where the inner closed loop becomes a double integrator, and for that a  $H_{PD}(s)$  controller is added.

#### 4. CASE STUDY

In this section, a case study will be considered for controlling the  $BIS(t)$  [%] in such a manner that it arrives at  $BIS = 50\%$ , most important without any overshoot and a steady-state error as small as possible.

According to the open source simulator the first step is to define values for the parameters of the model Ionescu et al. (2021). For the purpose of the present paper the system in (1) will be considered and let us define the following values for the vectorial functions:

$$f_1(\mathbf{x}) = \begin{bmatrix} -0.8436x_1(t) + 0.0735x_2(t) + 0.0035x_3(t) \\ 0.1841x_1(t) - 0.0735x_2(t) \\ 0.1958x_1(t) - 0.0035x_3(t) \\ 0.4560x_1(t) - 0.4560x_e(t) \end{bmatrix},$$

$$g_1(\mathbf{x}) = [1 \ 0 \ 0 \ 0]^T$$

and as for the parameters of the output function we have  $C_{50} = 4.6$ ;  $E_0 = 100$ ;  $E_m = 100$ ;  $\gamma = 10$ . This set of values will be referred to as *Patient 1*. In this case, as it has been previously described, the zero dynamics is stable. The diffeomorphism will be as presented in (7) therefore the closed-loop transfer function will be a double integrator

$$H(s) = \frac{1}{s^2}.$$

As seen in Fig. 2 the only block left is the  $H_{PD}(s)$ , imposing a certain structure for the closed loop that ensures no overshoot, the controller transfer function is computed as in (25):

$$H_{PD}(s) = \frac{0.1s}{s + 1.1}. \quad (25)$$

Fig. 3 show the controlled output BIS reaching the desired value of 50% with no overshoot and a steady-state error  $\varepsilon_p < 2\%$ .

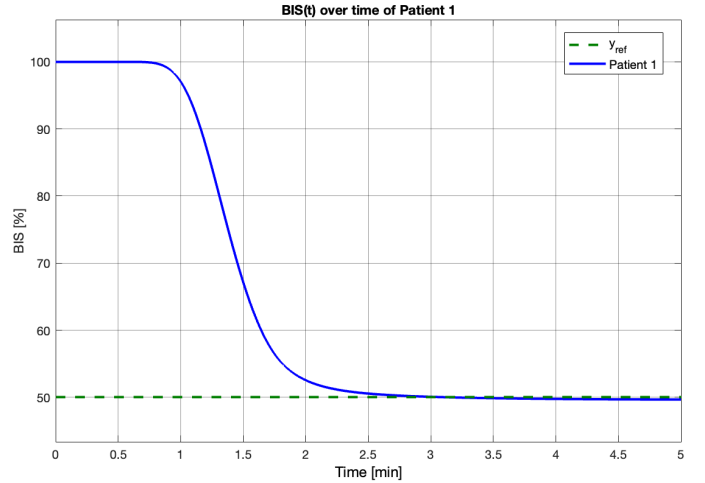


Fig. 3. The BIS of 1 patient

The proposed control strategy is model based. Thus it is necessary to analyse the robustness of the approach in the case of parameter variations due to patient intra/inter-variability.

To consider this case study complete let us take in consideration the next realisation of the system:

$$(\tilde{\Sigma}) : \begin{cases} \dot{\mathbf{x}} = f(\mathbf{x}) + \Delta f(\mathbf{x}) + g(\mathbf{x})u(t); \\ y(t) = h(\mathbf{x}), \end{cases} \quad (26)$$

where  $\Delta f(\mathbf{x})$  is the varying values of  $f(\mathbf{x})$  and their from can be described as parametric uncertainties smooth in their arguments. Let us take in consideration a varying range of  $\pm 10\%$  and map them onto the dynamics with a normal Gaussian distribution as presented in (27).

$$\begin{pmatrix} \mathbf{f} \\ \mathbf{g} \end{pmatrix} \sim \mathcal{N} \left( \begin{pmatrix} -10\% \\ 0 \end{pmatrix}, \begin{pmatrix} +10\% \\ 0 \end{pmatrix} \right) \quad (27)$$

$\underbrace{\hspace{1.5cm}}_{\min\{\Delta f(\mathbf{x})\}} \quad \underbrace{\hspace{1.5cm}}_{\max\{\Delta f(\mathbf{x})\}}$

For this now there will be  $\sigma$  sets of values for patients with the extreme varying values of  $\pm 10\%$  on which the control structure will be tested on. It is expected to have differences, given the model-based nature of the control structure. Considering model variations due to patient variability, the designed control signal  $u(t)$  may not ensure the exact linearization and the inner closed loop may begin to behave in an unpredictable manner.

Let us consider  $\sigma = 10$  therefore there will be 10 patients. The results can be seen in Fig. 4. It is important to notice that the nature of the signal does not change, it has no

unwanted dynamics, and most important for us, it has no overshoot.

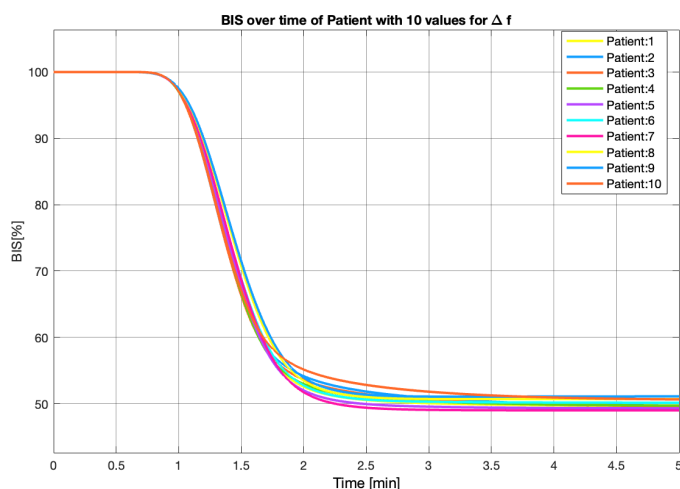


Fig. 4. The BIS of  $\sigma = 10$  patients

The only problem now is the steady-state error that can be seen in the results, this is due to the residual nonlinearities that are produced by  $\Delta f(\mathbf{x})$ , but is worth mentioning that the parametric uncertainties do not introduce dynamics of other nature, given the evolution of the system. This section concludes with the idea that the controller works within performance boundaries if the system has parametric uncertainties that can be included in a polytopic inclusion, or a convex hull under the normal distribution from (27).

## 5. CONCLUSION

The paper aimed to design a control law that takes the exact linearization of the model and ensures performances of no overshoot and minimum steady-state error for a system with no parametric uncertainties. The goal was achieved. Moreover we went at the extent of testing the control law on a system with parametric uncertainties and found that the performances are close to the first case. However this seeds the ideas for future works, where it is intended to design the control strategy with those parametric uncertainties in mind, adding a layer of robustness to the control law.

## 6. ACKNOWLEDGEMENT

This work was financed by a grant of the Romanian Ministry of Research, Innovation and Digitization, PNRR-III-C9-2022-I8, grant number 760068/23.05.2023. This work was funded in part by the European Research Council (ERC) Consolidator Grant AMICAS, grant agreement No. 101043225, 2022-2027. Funded by the European Union. Views and opinions expressed are however those of the author(s) only and do not necessarily reflect those of the European Union or the European Research Council Executive Agency. Neither the European Union nor the granting authority can be held responsible for them.

## REFERENCES

- Al-Rifai, Z. and Mulvey, D. (2016). Principles of total intravenous anaesthesia: basic pharmacokinetics and model descriptions. *Bja Education*, 16(3), 92–97.
- Beck, C.L. (2015). Modeling and control of pharmacodynamics. *European Journal of Control*, 24, 33–49.
- Blussé van Oud-Alblas, H.J., Brill, M.J., Peeters, M.Y., Tibboel, D., Danhof, M., and Knibbe, C.A. (2019). Population pharmacokinetic-pharmacodynamic model of propofol in adolescents undergoing scoliosis surgery with intraoperative wake-up test: a study using bispectral index and composite auditory evoked potentials as pharmacodynamic endpoints. *BMC anaesthesiology*, 19(1), 1–12.
- C. Rosow, P.M. (2001). Bispectral index monitoring. *Anesthesiol. Clin. N. Am.*, 947–966.
- Gambús, P.L. and Trocóniz, I.F. (2015). Pharmacokinetic–pharmacodynamic modelling in anaesthesia. *British journal of clinical pharmacology*, 79(1), 72–84.
- Ionescu, C.M., Neckebroek, M., Ghita, M., and Copot, D. (2021). An open source patient simulator for design and evaluation of computer based multiple drug dosing control for anesthetic and hemodynamic variables. *IEEE Access*, 9, 8680–8694.
- Isidori, A. (1985). *Nonlinear control systems: an introduction*. Berlin, Heidelberg: Springer Berlin Heidelberg.
- Kharisov, E., Beck, C.L., and Bloom, M. (2012). Control of patient response to anesthesia using  $\mathcal{L}_1$  adaptive methods. *IFAC Proceedings Volumes*, 45(18), 391–396.
- Merigo, L., Padula, F., Latronico, N., Paltenghi, M., and Visioli, A. (2019). Optimized pid control of propofol and remifentanyl coadministration for general anesthesia. *Communications in nonlinear science and numerical simulation*, 72, 194–212.
- Minto, C.F., Schnider, T.W., Egan, T.D., Youngs, E., Lemmens, H.J., Gambus, P.L., Billard, V., Hoke, J.F., Moore, K.H., Hermann, D.J., et al. (1997). Influence of age and gender on the pharmacokinetics and pharmacodynamics of remifentanyl: I. model development. *The Journal of the American Society of Anesthesiologists*, 86(1), 10–23.
- Morley, A., Derrick, J., Mainland, P., Lee, B., and Short, T. (2000). Closed loop control of anaesthesia: an assessment of the bispectral index as the target of control. *Anaesthesia*, 55(10), 953–959.
- Pintea, P.A. and Mihaly, V. (2023). Glucose level control in type 1 diabetes patients. In *2023 27th International Conference on System Theory, Control and Computing (ICSTCC)*, 203–208. doi: 10.1109/ICSTCC59206.2023.10308454.
- Soltész, K., van Heusden, K., and Dumont, G. (2020). Models for control of intravenous anesthesia. *Copot, D., Automated Drug Delivery in Anesthesia*, 119–166.
- Struys, M.M., De Smet, T., Greenwald, S., Absalom, A.R., Bingé, S., and Mortier, E.P. (2004). Performance evaluation of two published closed-loop control systems using bispectral index monitoring: a simulation study. *The Journal of the American Society of Anesthesiologists*, 100(3), 640–647.
- Zhusubaliyev, Z.T., Medvedev, A., and Silva, M.M. (2015). Bifurcation analysis of pid-controlled neuromuscular blockade in closed-loop anesthesia. *Journal of Process Control*, 25, 152–163.